

EFFECT OF COOLING RATE ON THE SOLIDIFICATION BEHAVIOR OF AC AlSi₇Cu₂ ALLOY

This paper describes the effect of cooling rate on the size of the grains, SDAS and thermal characteristic results of the AC AlSi₇Cu₂ cast alloy. The solidification process was studied using the cooling curve and crystallization curve at solidification rate ranging from 0,16 up to 0,71 °C·s⁻¹. It was determined that higher solidification rate increases the aluminum dendrite nucleation temperature and solid fraction at the dendrite coherency point, which implies that mass feeding is extended. In addition, it was observed that the non-equilibrium solidus temperature and the size of the grains, SDAS constituent decreases when the solidification rate increases.

Описывается влияние скорости охлаждения на величину зерна, расстояние между осями вторичных дендритов и вытекающей термической характеристики литейного сплава AC AlSi₇Cu₂. Процесс кристаллизации был изучен с использованием кривой охлаждения и кривой кристаллизации при скорости кристаллизации в пределах от 0,16 до 0,71 °C·с⁻¹. Было определено, что более высокая скорость кристаллизации увеличивает температуру зарождения кристаллов дендритов алюминия и твердую фазу в точке когерентности дендритов, что подразумевает увеличение подаваемой массы. Наблюдалось, что неравновесная температура перехода в твердое состояние и размер зерен, расстояние между осями вторичных дендритов уменьшаются при увеличении скорости кристаллизации.

Introduction

High purity AlSiCu hypoeutectic alloys exhibit three main solidification reactions during the solidification process, starting with the formation of aluminum dendrites followed by the development of two main eutectic phases. The presence of alloying and impurity elements such as: Cu, Mg, Mn, Fe leads to more complex constituents (including intermetallic) that are characterized by metallographic techniques. Bäckerud et al. [4, 6, 7, 8] identified the reactions in AC AlSiXCuX, (3XX) alloys and listed four solid state phases, Table 1.

Table 1. Reactions occurring during the solidification of the AC AlSiXCuX, (3XX) alloys according to 4, 6, 7, 8

No	Reaction	Temperature [°C]
1	Development of dendritic network	620÷580
2	$L \rightarrow \alpha + \beta + AlFe_5Si$	570÷555
3	$L \rightarrow \alpha + \beta + Al_8FeMg_3Si_6 + Mg_2Si$	540÷500
4	$L \rightarrow \alpha + Al_2Cu + \beta + Al_5Cu_2Mg_8Si_6$	500÷470

The solidification path for AC AlSiXCuX, (3XX) alloy can be described:

1. A primary α -aluminum network forms between 620÷580 °C. The exact temperature depends mainly on the amount of Si and Cu concentration in the alloy.

2. Within the 570÷555 °C the eutectic mixture of Si and α -aluminum forms, leading to a further localized increase in Cu content of the remaining liquid. The Fe rich phases can also precipitate in this temperature range.

3. At approximately 540 °C the Mg₂Si and Al₈Mg₃FeSi₆ phases begin to precipitate.

4. A reduction in the temperature allows for precipitation of Al₂Cu and Al₁₅Mg₈Cu₂Si₆ phases between 500÷470 °C.

A comprehensive understanding of the solidification processes of the investigated industrial grade alloys requires the addition of grain refiners and eutectic Si modifiers using elements like: Ti, B, Sr, Na, Sb. Grain refiners that

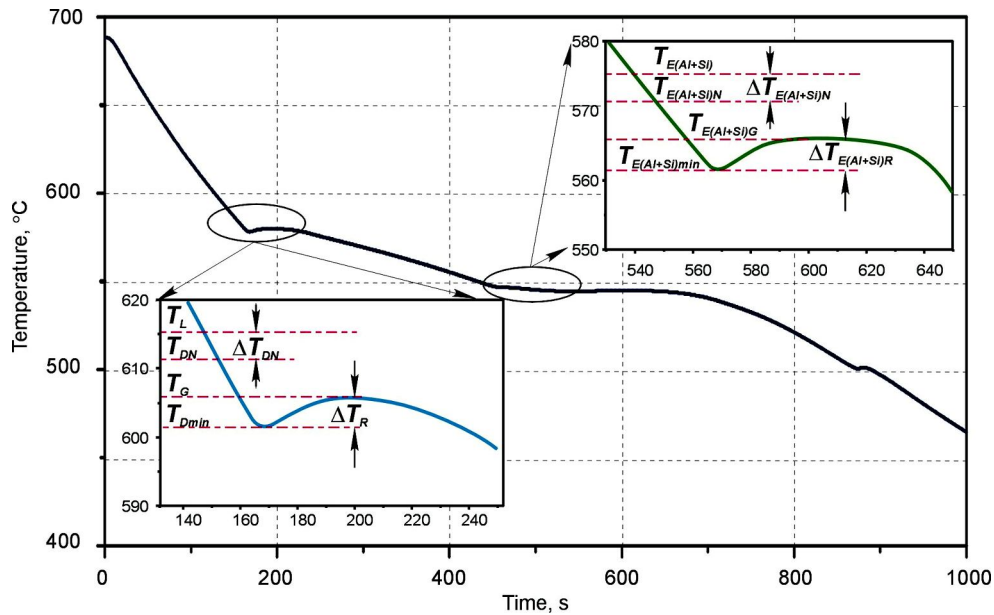


Figure 1. Generic AC AlSi₇Cu₂ alloy cooling curve obtained under the authors non-equilibrium experimental

affect the morphology of the nucleating grains. Commercial aluminum alloys contain a limited number of active nucleating particles. In addition, these particles have a poor nucleating potency, therefore the melt requires a high degree of undercooling ($\Delta T_{DN} \approx 3 \div 5$ °C, see Figure 1) before these particles become active. Therefore, the effective melt processing requires the addition of grain refiners like the Al 3 %Ti 3 %B master alloy. This master alloy contains a large number of insoluble boride particles, which effectively nucleate a great number of aluminum grains. Grain refiners added to the melt produce changes in the following thermal characteristics:

- The nucleation occurs far above the bulk equilibrium temperature T_L , for the liquidus temperature for alloys without grain modifiers (please refer to Figure 1).

- There is no undercooling before the actual growth temperature is reached (the recalescence effect is not present, $\Delta T_R \approx 0$ °C, see Figure 1) [8, 9].

Silicon modifiers (Sr, Na and Sb just to mention the most popular ones) change the morphology of the eutectic silicon crystals from large flakes into fibrous structures resembling a coral like morphology. The growth process of the eutectic silicon crystals is influenced by

these additions, and the $\alpha + \beta$ eutectic reaction temperature is lowered by $5 \div 10$ °C [8].

Experimental procedure

The experimental alloy used in this investigation was prepared at the University of Windsor (Canada) in the Light Metals Casting Laboratory, by mixing the AC AlSi₅Cu₁(Mg) (C 355.2) commercial alloys and two master alloys AlSi₄₉ and AlCu₅₅, in a 10 kg capacity ceramic crucible. The melted test samples were held for 12 hours in Lindberg™ electric resistance furnace at 850 ± 5 °C under a protective argon gas atmosphere. Before casting the melts were homogenized and degassed with the aim to reduce the hydrogen level below $0,100 \pm 0,005$ ml H₂/100 g of aluminum and the surface was carefully skimmed. A total of 24 samples of the AC AlSi₇Cu₂ alloy were prepared and this chemical compositions was analyzed by Optical Emission Spectroscopy (OES) as per the ASTM E1251 specification. The chemical compositions of this alloys is given in Table 2.

Thermal analysis (TA) tests were conducted using the UMSA Technology Platform 10 developed at the University of Windsor in collaboration with the Silesian University of Technology. The TA test samples were cast into a 0,25 mm thick stainless steel cap. The cup was

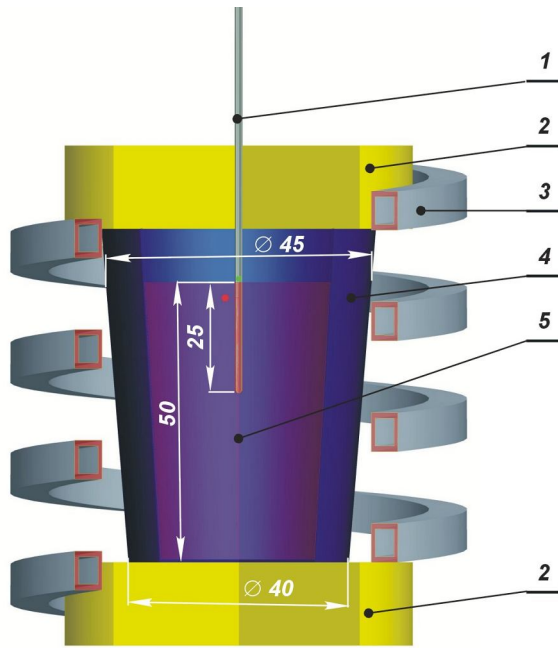


Figure 2. Schematic of the UMSA Thermal Analysis Platform experimental set-up: 1 – low thermal mass thermocouple, 2 – thermal insulation, 3 – heating and cooling coil, 4 – steel cup, 5 – test sample

isolated at the top and bottom to allow for Newtonian type heat transfer only. A schematic of the experimental set-up for thermal analysis is depicted in Figure 2. In order to obtain statistical confidence, the TA experiments were repeated eight times for each time.

Table 2. Average chemical composition (wt %) of investigated alloy, equilibrium liquidus temperature – T_L and cooling rate – CR applied in the investigation

Si	Fe	Cu	Mn	Mg	Zn	Ti	Sr	T_L , [°C]	CR, [°C·s ⁻¹]
6,982	0,168	1,91	0,110	0,255	0,425	0,090	0,003	612	0,16
									0,33
									0,71

The cooling curve parameters considered in this work schematically depicted in Figure 1 where: the equilibrium liquidus temperature T_L that was calculated by the JMatPro software. The aluminum dendritic network nucleation temperature T_{DN} , the $\alpha + \beta$ eutectic nucleation temperature $T_{E(Al+Si)N}$, the temperature where the new dendritic crystals have grown T_{Dmin} , the temperature where the new silicon crystals have

grown $T_{E(Al+Si)min}$, were calculated using the first derivative of the cooling curve. The equilibrium liquidus temperature T_L and equilibrium eutectic temperature $T_{E(Al+Si)}$ were used like reference point for calculation of the appropriate: α -aluminum phases nucleation undercooling ΔT_{DN} , and $\alpha + \beta$ eutectic nucleation undercooling $\Delta T_{E(Al+Si)N}$. The UMSA test analysis samples were cut longitudinally and then sectioned horizontally approximately 15 mm from the bottom and were prepared for metallographic analysis using standard procedures. Metallographic specimens were etched using 0,5 % HF and a Keller & Dix etching solution.

Discussion of experimental results

Figure 3 shows the variation of the α -aluminum (Al_{DEN}) nucleation temperature as a function of cooling rate and the variation of the Al_{DEN} nucleation undercooling and recalescence temperature. Standard errors calculated for each measured data point also have been included in the graph. It is evidence from the plot, that the Al_{DEN} nucleation temperature increase with increase cooling rate in the range of cooling rate studied here. Due to the increase the cooling rate the nucleation undercooling decrease. The phenomena of an increase in the nucleation temperature with an increase in the solidification rate depends on the mobility of the clusters of atoms in the melt. These groups of the froze atoms produces the fluctuation clusters and fluctuation embryos, which are the nucleation primers.

The increase of the cooling rate with an increase amount of the nucleation primers and reduction of the recalescence temperature is well established fact. This effect have influence on the grain size. Figure 4 shows the variation of the grain size and secondary dendrite arm spacing (SDAS) as a function of cooling rate. As seen on the picture the increase cooling rate decrease strongly the grain size and SDAS. Three micrographs from samples AC AlSi₇Cu₂ alloy cooled with cooling rate: 0,16 °C·s⁻¹, 0,46 °C·s⁻¹ and 0,72 °C·s⁻¹ are show in Figure 5. The reduction of (SDAS) is clearly evident from this pictures. This variation has been showed graphically in Figure 4. SDAS is stricte depending on the cooling rate. In the highest coolingrate, the SDAS is fine ($\approx 36,6 \mu\text{m}$) and

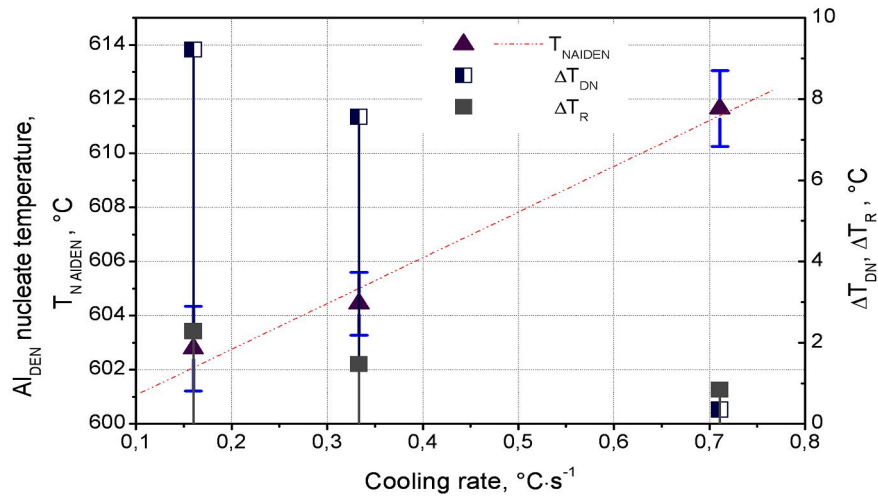


Figure 3. Variation of the Al_{DEN} nucleate temperature and the Al_{DEN} nucleate undercooling and recalescence temperature as a function of cooling rate

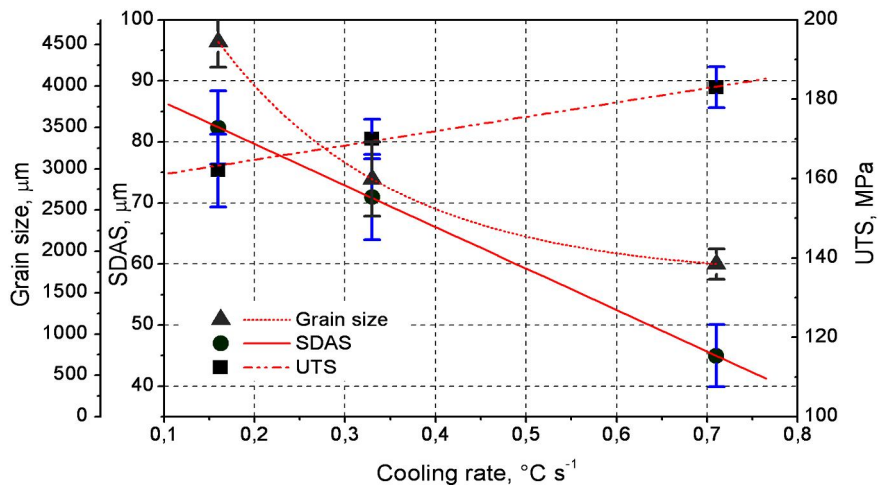


Figure 4. Variation of the grain size SDAS and UTS as a function of cooling rate

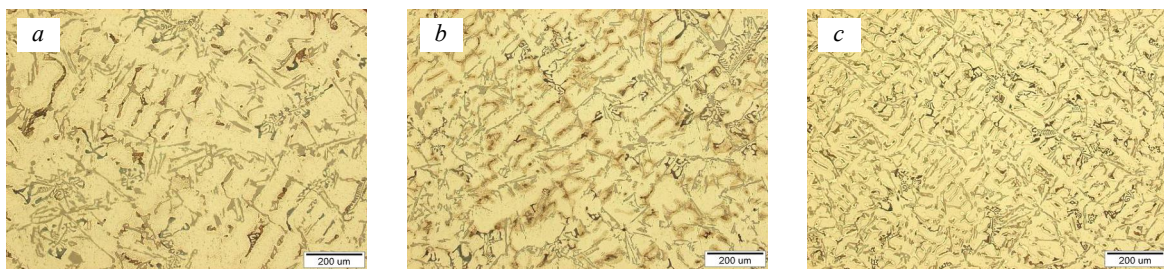


Figure 5. Micrographs revealing the microstructures of AC $AlSi_7Cu_2$ that solidified: a) $0,16 \text{ } ^\circ\text{C}\cdot\text{s}^{-1}$; b) $0,46 \text{ } ^\circ\text{C}\cdot\text{s}^{-1}$; c) $0,72 \text{ } ^\circ\text{C}\cdot\text{s}^{-1}$

easily visible. For the sample that was cooled with lowest cooling rate, the SDAS is large ($\approx 87,06 \text{ } \mu\text{m}$). Therefore the alloy's design and process engineers have a wide range of solidification rates (process parameters) to chose from.

There have been a many studies on aluminum alloys reported to data 1, 2, 5. According to these studies, the mechanical properties of the aluminum alloys are strongly dependent on the effect of SDAS. Tensile properties increase

with a decrease the SDAS. Investigations results shows, the increase the cooling rate from $0,16\text{ }^{\circ}\text{C}\cdot\text{s}^{-1}$ to $0,72\text{ }^{\circ}\text{C}\cdot\text{s}^{-1}$ influence on the reduction of the SDAS, what have influence on the ultimate tensile strength (UTS). The UTS increase from 162 MPa for lowest cooling rate to 183 MPa for highest cooling rate (Figure 5).

Conclusion

An increase in the solidification rate leads to an increase in the Al_{DEN} nucleation temperature and a decrease in the recalescence temperature of the dendrite formation. These phenomena lead to an increased number of nucleus that affect the size of the grains and the Secondary Dendrite Arm Spacing (SDAS). The SDAS and the grain size can be assessed by measurement of the Al_{DEN} nucleation temperature, the Al_{DEN} undercooling, and the recalescence temperature.

REFERENCES

1. *L.A. Dobrzański, K. Labisz, R. Maniara*, Proceedings of the 13th International Scientific Conference, Gliwice-Wisła, 2005.
2. *Z. Li, A.M. Samuel, F.H. Samuel, C. Ravindran, S. Valtierra, H.W. Daty*, Materials Science and Engineering, 2003.
3. *R. MacKay, M. Djurdjevic, J.H. Sokolowski*, AFS Transaction, 2000.
4. *C.H. Cáceres, M.B. Djurdjevic, T.J. Stockwell*, Scripta Materiala, 1999.
5. *J.M. Boileau, J.W. Zindel and J.E. Allison*, Society of Automotive Engineers, Inc., 1997.
6. *A.M. Samuel, A. Gotmare, F.H. Samuel*, Composite Science and Technology, 1994.
7. *L. Bäckerud, E. Król, J. Tamminen*: Solidification Characteristics of Aluminum Alloys, Vol. 1, Universitetsforlaget, Oslo, 1986.
8. *L. Bäckerud, G. Chai, J. Tamminen*: Solidification Characteristics of Aluminum Alloys, Vol. 2., AFS, 1992.
9. *L. Bäckerud, G. Chai*: Solidification Characteristics of Aluminum Alloys, Vol. 3, AFS, 1992.
10. <http://www.uwindsor.ca/umsa>